

Quark-Hadron Duality in Spin Structure Functions g_1^p and g_1^d

P.E. Bosted,^{37,*} K.V. Dharmawardane,^{30,†} G.E. Dodge,³⁰ T.A. Forest,³⁰ S.E. Kuhn,³⁰
Y. Prok,^{40,‡} G. Adams,³² M. Amarian,³⁰ P. Ambrozewicz,¹² M. Anghinolfi,¹⁸ G. Asryan,⁴²
H. Avakian,^{17,37} H. Bagdasaryan,^{42,30} N. Baillie,⁴¹ J.P. Ball,² N.A. Baltzell,³⁶ S. Barrow,¹³
V. Batourine,²³ M. Battaglieri,¹⁸ K. Beard,²² I. Bedlinskiy,²¹ M. Bektasoglu,³⁰ M. Bellis,^{32,5}
N. Benmouna,¹⁴ A.S. Biselli,¹¹ B.E. Bonner,³³ S. Bouchigny,^{37,19} S. Boiarinov,^{21,37}
R. Bradford,⁵ D. Branford,¹⁰ W.K. Brooks,³⁷ S. Bültmann,³⁰ V.D. Burkert,³⁷
C. Butuceanu,⁴¹ J.R. Calarco,²⁷ S.L. Careccia,³⁰ D.S. Carman,²⁹ B. Carnahan,⁶
A. Cazes,³⁶ S. Chen,¹³ P.L. Cole,^{37,16} P. Collins,² P. Coltharp,¹³ D. Cords,^{37,§}
P. Corvisiero,¹⁸ D. Crabb,⁴⁰ H. Crannell,⁶ V. Crede,¹³ J.P. Cummings,³² R. De Masi,⁷
R. DeVita,¹⁸ E. De Sanctis,¹⁷ P.V. Degtyarenko,³⁷ H. Denizli,³¹ L. Dennis,¹³ A. Deur,³⁷
C. Djalali,³⁶ J. Donnelly,¹⁵ D. Doughty,^{8,37} P. Dragovitsch,¹³ M. Dugger,² S. Dytman,³¹
O.P. Dzyubak,³⁶ H. Egiyan,^{41,37,¶} K.S. Egiyan,⁴² L. Elouadrhiri,^{8,37} P. Eugenio,¹³
R. Fatemi,⁴⁰ G. Fedotov,²⁶ R.J. Feuerbach,⁵ H. Funsten,⁴¹ M. Garçon,⁷ G. Gavalian,^{27,30}
G.P. Gilfoyle,³⁵ K.L. Giovanetti,²² F.X. Girod,⁷ J.T. Goetz,³ E. Golovatch,^{18,**}
A. Gonenc,¹² R.W. Gothe,³⁶ K.A. Griffioen,⁴¹ M. Guidal,¹⁹ M. Guillo,³⁶ N. Guler,³⁰
L. Guo,³⁷ V. Gyurjyan,³⁷ C. Hadjidakis,¹⁹ K. Hafidi,¹ R.S. Hakobyan,⁶ J. Hardie,^{8,37}
D. Heddle,^{8,37} F.W. Hersman,²⁷ K. Hicks,²⁹ I. Hleiqawi,²⁹ M. Holtrop,²⁷ M. Huertas,³⁶
C.E. Hyde-Wright,³⁰ Y. Ilieva,¹⁴ D.G. Ireland,¹⁵ B.S. Ishkhanov,²⁶ E.L. Isupov,²⁶
M.M. Ito,³⁷ D. Jenkins,³⁹ H.S. Jo,¹⁹ K. Joo,⁹ H.G. Juengst,³⁰ C. Keith,³⁷ J.D. Kellie,¹⁵
M. Khandaker,²⁸ K.Y. Kim,³¹ K. Kim,²³ W. Kim,²³ A. Klein,^{30,††} F.J. Klein,^{12,6}
M. Klusman,³² M. Kossov,²¹ L.H. Kramer,^{12,37} V. Kubarovsky,³² J. Kuhn,^{32,5}
S.V. Kuleshov,²¹ J. Lachniet,^{5,30} J.M. Laget,^{7,37} J. Langheinrich,³⁶ D. Lawrence,²⁵
Ji Li,³² A.C.S. Lima,¹⁴ K. Livingston,¹⁵ H. Lu,³⁶ K. Lukashin,⁶ M. MacCormick,¹⁹
J.J. Manak,³⁷ N. Markov,⁹ S. McAleer,¹³ B. McKinnon,¹⁵ J.W.C. McNabb,⁵
B.A. Mecking,³⁷ M.D. Mestayer,³⁷ C.A. Meyer,⁵ T. Mibe,²⁹ K. Mikhailov,²¹ R. Minehart,⁴⁰
M. Mirazita,¹⁷ R. Miskimen,²⁵ V. Mokeev,²⁶ L. Morand,⁷ S.A. Morrow,^{19,7}
M. Moteabbed,¹² J. Mueller,³¹ G.S. Mutchler,³³ P. Nadel-Turonski,¹⁴ J. Napolitano,³²
R. Nasseripour,^{12,36} S. Niccolai,^{14,19} G. Niculescu,²² I. Niculescu,^{14,22} B.B. Niczyporuk,³⁷
M.R. Niroula,³⁰ R.A. Niyazov,^{30,37} M. Nozar,³⁷ G.V. O’Rielly,¹⁴ M. Osipenko,^{18,26}

A.I. Ostrovidov,¹³ K. Park,²³ E. Pasyuk,² C. Paterson,¹⁵ S.A. Philips,¹⁴ J. Pierce,⁴⁰
 N. Pivnyuk,²¹ D. Pocanic,⁴⁰ O. Pogorelko,²¹ E. Polli,¹⁷ S. Pozdniakov,²¹ B.M. Preedom,³⁶
 J.W. Price,⁴ D. Protopopescu,^{27,15} L.M. Qin,³⁰ B.A. Raue,^{12,37} G. Riccardi,¹³
 G. Ricco,¹⁸ M. Ripani,¹⁸ F. Ronchetti,¹⁷ G. Rosner,¹⁵ P. Rossi,¹⁷ D. Rowntree,²⁴
 P.D. Rubin,³⁵ F. Sabatié,^{30,7} C. Salgado,²⁸ J.P. Santoro,^{39,37,‡‡} V. Sapunenko,^{18,37}
 R.A. Schumacher,⁵ V.S. Serov,²¹ Y.G. Sharabian,³⁷ J. Shaw,²⁵ N.V. Shvedunov,²⁶
 A.V. Skabelin,²⁴ E.S. Smith,³⁷ L.C. Smith,⁴⁰ D.I. Sober,⁶ A. Stavinsky,²¹ S.S. Stepanyan,²³
 S. Stepanyan,^{37,8,42} B.E. Stokes,¹³ P. Stoler,³² S. Strauch,³⁶ R. Suleiman,²⁴ M. Taiuti,¹⁸
 S. Taylor,³³ D.J. Tedeschi,³⁶ U. Thoma,^{37,§§} R. Thompson,³¹ A. Tkabladze,¹⁴
 S. Tkachenko,³⁰ L. Todor,⁵ C. Tur,³⁶ M. Ungaro,⁹ M.F. Vineyard,^{38,35} A.V. Vlassov,²¹
 L.B. Weinstein,³⁰ D.P. Weygand,³⁷ M. Williams,⁵ E. Wolin,³⁷ M.H. Wood,^{36,¶¶}
 A. Yegneswaran,³⁷ J. Yun,³⁰ L. Zana,²⁷ J. Zhang,³⁰ B. Zhao,⁹ and Z. Zhao³⁶

(The CLAS Collaboration)

¹*Argonne National Laboratory, Argonne, Illinois 60439*

²*Arizona State University, Tempe, Arizona 85287-1504*

³*University of California at Los Angeles, Los Angeles, California 90095-1547*

⁴*California State University, Dominguez Hills, Carson, CA 90747*

⁵*Carnegie Mellon University, Pittsburgh, Pennsylvania 15213*

⁶*Catholic University of America, Washington, D.C. 20064*

⁷*CEA-Saclay, Service de Physique Nucléaire, F91191 Gif-sur-Yvette, France*

⁸*Christopher Newport University, Newport News, Virginia 23606*

⁹*University of Connecticut, Storrs, Connecticut 06269*

¹⁰*Edinburgh University, Edinburgh EH9 3JZ, United Kingdom*

¹¹*Fairfield University, Fairfield, CT 06824*

¹²*Florida International University, Miami, Florida 33199*

¹³*Florida State University, Tallahassee, Florida 32306*

¹⁴*The George Washington University, Washington, DC 20052*

¹⁵*University of Glasgow, Glasgow G12 8QQ, United Kingdom*

¹⁶*Idaho State University, Pocatello, Idaho 83209*

¹⁷*INFN, Laboratori Nazionali di Frascati, 00044 Frascati, Italy*

- ¹⁸*INFN, Sezione di Genova, 16146 Genova, Italy*
- ¹⁹*Institut de Physique Nucleaire ORSAY, Orsay, France*
- ²⁰*Institute für Strahlen und Kernphysik, Universität Bonn, Germany*
- ²¹*Institute of Theoretical and Experimental Physics, Moscow, 117259, Russia*
- ²²*James Madison University, Harrisonburg, Virginia 22807*
- ²³*Kyungpook National University, Daegu 702-701, South Korea*
- ²⁴*Massachusetts Institute of Technology, Cambridge, Massachusetts 02139-4307*
- ²⁵*University of Massachusetts, Amherst, Massachusetts 01003*
- ²⁶*Moscow State University, General Nuclear Physics Institute, 119899 Moscow, Russia*
- ²⁷*University of New Hampshire, Durham, New Hampshire 03824-3568*
- ²⁸*Norfolk State University, Norfolk, Virginia 23504*
- ²⁹*Ohio University, Athens, Ohio 45701*
- ³⁰*Old Dominion University, Norfolk, Virginia 23529*
- ³¹*University of Pittsburgh, Pittsburgh, Pennsylvania 15260*
- ³²*Rensselaer Polytechnic Institute, Troy, New York 12180-3590*
- ³³*Rice University, Houston, Texas 77005-1892*
- ³⁴*Sakarya University, Sakarya, Turkey*
- ³⁵*University of Richmond, Richmond, Virginia 23173*
- ³⁶*University of South Carolina, Columbia, South Carolina 29208*
- ³⁷*Thomas Jefferson National Accelerator Facility, Newport News, Virginia 23606*
- ³⁸*Union College, Schenectady, NY 12308*
- ³⁹*Virginia Polytechnic Institute and State University, Blacksburg, Virginia 24061-0435*
- ⁴⁰*University of Virginia, Charlottesville, Virginia 22901*
- ⁴¹*College of William and Mary, Williamsburg, Virginia 23187-8795*
- ⁴²*Yerevan Physics Institute, 375036 Yerevan, Armenia*

(Dated: February 2, 2008)

Abstract

New measurements of the spin structure functions of the proton and deuteron $g_1^p(x, Q^2)$ and $g_1^d(x, Q^2)$ in the nucleon resonance region are compared with extrapolations of target-mass-corrected next-to-leading-order (NLO) QCD fits to higher energy data. Averaged over the entire resonance region ($W < 2$ GeV), the data and QCD fits are in good agreement in both magnitude and Q^2 dependence for $Q^2 > 1.7$ GeV²/c². This “global” duality appears to result from cancellations among the prominent “local” resonance regions: in particular strong $\sigma_{3/2}$ contributions in the $\Delta(1232)$ region appear to be compensated by strong $\sigma_{1/2}$ contributions in the resonance region centered on 1.5 GeV. These results are encouraging for the extension of NLO QCD fits to lower W and Q^2 than have been used previously.

PACS numbers: 13.60.Hb, 25.30.Fj, 24.30.Gd

The theoretical description of particle interactions has utilized quark-gluon degrees of freedom at high energies and hadronic degrees of freedom at low energies. With suitable averaging over resonant excitations, the two approaches have been found in several cases to be nearly equivalent, a phenomenon referred to as quark-hadron duality. These cases include e^+e^- annihilation, semi-leptonic decays of heavy mesons, electron-pion scattering, semi-inclusive deep-inelastic scattering, and both spin-averaged and spin-dependent inclusive lepton-nucleus scattering [1], the subject of the present investigation. Pragmatically, understanding the limitations and applicability of quark-hadron duality in this process is useful in order to define the kinematic region in which parton distribution functions (PDF) can be reliably extracted.

In lepton-nucleon scattering, the low and high energy regimes have traditionally been separated using W , the invariant mass of the hadronic final state, and Q^2 , the four momentum transfer squared. A region of prominent nucleon resonances is observed for $W < 2$ GeV and $Q^2 < 10$ GeV²/c², while for higher W or Q^2 there is no longer any obvious resonance structure. Historically, quark-hadron duality was first observed in 1970 by Bloom and Gilman [2] in the spin-averaged lepton-nucleon process. They noted that the inclusive structure function, $F_2(W, Q^2)$ averages smoothly at low W and Q^2 to the scaling function $F_2(W, Q^2)$ measured at high energy, using an empirical scaling variable in place of the original Bjorken x scaling variable. Subsequently, Georgi and Politzer [3] found that quark-hadron duality is exhibited down to $Q^2 \sim 1$ GeV²/c² using the Nachtmann [4] scaling variable $\xi \equiv 2x/(1 + \sqrt{1 + 4M^2x^2/Q^2})$ which approximates the purely kinematic higher twist corrections arising from the non-zero nucleon mass M . More recently, explicit target-mass (TM) corrections have been derived in the framework of QCD for both unpolarized and polarized structure functions [5] that obviate the need for an approximate scaling variable.

To explain quark-hadron duality theoretically, de Rújula, Georgi, and Politzer [6] employed a perturbative operator product expansion of QCD structure function moments. In this framework, quark-hadron duality implies a small net effect from higher twist contributions, once the kinematic target-mass contribution is taken into account. In a simple QCD picture, the additional higher twist contributions (which are proportional to powers of $1/\sqrt{Q^2}$) are due to quark-quark and quark-gluon correlations. Close and Isgur [7] provided an interesting explanation in the constituent quark model in terms of cancellations from resonance contributions with opposite parity. A recent theoretical QCD study [8] of both

polarized and unpolarized structure functions incorporates many of these concepts, with the addition of a careful treatment of so-called high- x resummation corrections. The authors concluded that higher-twist corrections are suppressed more for the unpolarized structure function F_2 than for the proton polarized structure function g_1^p , where a sizable negative contribution is observed. A comprehensive review of quark-hadron duality from both the experimental and theoretical perspective was also published recently [1].

Unpolarized structure function data exhibit excitation-energy-averaged scaling not only averaged over the entire resonance region ($M < W < 2$ GeV), referred to as “global duality”, but also in each of several restricted regions in W , corresponding to the three prominent resonance regions centered on $W = 1.23, 1.5$ and 1.7 GeV, a phenomenon referred to as “local duality”. This was demonstrated experimentally using high-statistical-accuracy data from Jefferson Lab [10], and interpreted theoretically by Carlson and Mukhopadhyay [11] using the expected pQCD Q^2 -dependence of nucleon transition form factors.

The new data presented in this report augment previously available results for g_1^p from SLAC [12, 13], DESY [14] and JLab [15, 16] with higher statistical precision and an expanded range of Q^2 . This allows us to experimentally examine local duality for g_1^p much more accurately than was previously possible. The addition of a considerable body of deuteron g_1^d data allows the first examination of the isospin dependence of global duality in g_1 .

When testing duality there is an intrinsic uncertainty as to which DIS curves to use for comparison with the averaged resonance region data. In this paper, we choose the average of two representative Next-to-Leading Order (NLO) QCD fits [17, 18] to polarized structure function data above the resonance region. The NLO evolution is considered to be reasonably reliable down to Q^2 values of order $1 \text{ GeV}^2/c^2$. We choose to use fits with NLO evolution, rather than LO or purely empirical fits to data, to give the best possible estimate of the Q^2 -dependence of g_1 . The high-energy data used in the NLO QCD fits have relatively large errors compared to those for unpolarized structure functions, particularly at high values of x that tend to correspond to our resonance region data. Since precise error bands in our kinematic region are not available, we ascribe a very approximate relative error of 10% (20%) to the g_1^p (g_1^d) DIS fits, independent of x . The error on the average deuteron DIS fit is larger due to the much larger relative contribution of negatively polarized quarks in the neutron compared to the proton. We take kinematic target-mass corrections into account

using the prescription of Blümlein and Tkabladze [5]:

$$\begin{aligned}
g_1^{TM}(x, Q^2) &= \frac{x}{\xi(1+\gamma)^{3/2}} g_1^{QCD}(\xi, Q^2) \\
&+ \frac{(x+\xi)\gamma}{\xi(1+\gamma)^2} \int_{\xi}^1 \frac{du}{u} g_1^{QCD}(u, Q^2) \\
&- \frac{\gamma(2-\gamma)}{2(1+\gamma)^{5/2}} \int_{\xi}^1 \frac{du}{u} \int_u^1 \frac{dv}{v} g_1^{QCD}(v, Q^2),
\end{aligned} \tag{1}$$

where $\gamma = 4M^2x^2/Q^2$. This prescription is not unique, and in particular has the drawback of resulting in non-zero values of g_1 at $x = 1$. An approach that avoids this problem has been worked out for F_2 [19], but is not yet available for g_1 . The calculation of high- x resummation corrections is theoretically more complicated [9] and technically more challenging than target mass corrections. Rather than attempting these calculations ourselves, we simply note that Ref. [8] finds enhancements of order 10% to 20% for the proton averaged over the full resonance region, roughly independent of Q^2 for $0.5 < Q^2 < 5 \text{ GeV}^2/c^2$. This corrections could well be different for the deuteron and for individual “local” regions in W .

The analysis is based on recently published data [20] from Jefferson Lab. Very briefly, in this experiment the CEBAF Large Acceptance Spectrometer [21] in Jefferson Lab’s Hall B was used to measure spin asymmetries in the scattering of longitudinally polarized electrons from longitudinally polarized protons and deuterons. The data were collected in 2001 using incident energies of 1.6 GeV and 5.7 GeV. Beam currents ranged from 1 to 5 nA, and the beam polarization averaged 70%. The detector package [21] allowed clean identification of electrons scattered at polar angles between 8 and 45 degrees. Ammonia, polarized via Dynamic Nuclear Polarization [22], was used to provide polarized protons and deuterons, using the $^{15}\text{NH}_3$ and $^{15}\text{ND}_3$ isotopes, respectively. The average target polarization was about 75% for the proton and about 25% for the deuteron. The data were divided into 40 bins in Q^2 , equally spaced on a logarithmic scale between 0.01 and 10 GeV^2/c^2 .

Values of $g_1(x, Q^2)$ were determined from the ratios of g_1/F_1 presented in [20] using recent fits to proton [23] and deuteron [24] data to evaluate the unpolarized structure function $F_1(x, Q^2)$. The resulting values of $g_1(x, Q^2)$ for both the proton and the deuteron are plotted (scaled by x) as a function of x for four representative Q^2 bins in Figure 1. The three arrows on each panel correspond to the three prominent resonance regions at $W = 1.7, 1.5,$ and 1.23 GeV , from left to right. We compare the data to the extrapolations of DIS fits (as described above), represented by the hatched bands.

It can be seen in Fig. 1 that the data in fixed Q^2 bins indeed exhibit oscillations in x compared to the smooth behavior of the DIS curves. In addition, the averaged data become increasingly commensurate with the models with increasing Q^2 , as expected if quark-hadron duality is valid for g_1 . In closer detail, one can also observe that the experimental data for both the proton and the deuteron lie below the curves in the $\Delta(1232)$ region, and above in the $W = 1.5$ GeV [$S_{11}(1535)/D_{13}(1520)/P_{11}(1440)$] region. This is not surprising at low to moderate Q^2 , where resonant contributions dominate over non-resonant contributions. Recall that g_1 is proportional to $\sigma_{1/2} - \sigma_{3/2}$. The $N \rightarrow \Delta(1232)$ is known to be dominated by M1 strength [25] over the Q^2 range of the present study, which results in a virtual photon cross section $\sigma_{3/2}$ about three times larger than $\sigma_{1/2}$, corresponding to negative values of g_1 . In contrast, in the DIS limit of incoherent scattering from massless quarks, g_1 must be positive due to helicity conservation. In the second resonance region, the $S_{11}(1535)$ and $P_{11}(1440)$ transitions can only contribute to $\sigma_{1/2}$, and recent studies [26] show that the $N \rightarrow D_{13}(1520)$ changes from dominantly $\sigma_{3/2}$ at low Q^2 to dominantly $\sigma_{1/2}$ above 1 GeV $^2/c^2$. The three resonances together therefore are expected to result in large positive values of g_1 above 1 GeV $^2/c^2$ (potentially larger than the DIS limit).

To clarify these observations with respect to both local and global duality, we have averaged over x both data and models for g_1 over a Q^2 -dependent interval corresponding to four specific regions in W . The x -averaged values of g_1 for the entire resonance region (scaled by Q^2) are plotted as a function of Q^2 in Fig. 2 for both targets. The proton averages for four smaller regions in W are plotted in Fig. 3. Specifically, the averages were determined as

$$\langle g_1(Q^2) \rangle = \frac{\int_{x_l}^{x_h} g_1(x, Q^2) dx}{x_h - x_l},$$

where x_l and x_h correspond respectively to the maximum and minimum values of W in the interval considered, at the given value of Q^2 [using the definition $x^{-1} = 1 + (W^2 - M^2)/Q^2$]. The TM-corrected NLO PDF parameterizations shown in Fig. 1 were averaged in the same way as for the experimental data.

The averages displayed in Figs. 2 test “global” duality by averaging g_1 over x for the entire region from pion threshold to $W = 2$ GeV. The data for both targets exhibit a power-law-type deviation from the DIS curves at low Q^2 , but essentially agree with them above $Q^2 = 1.7$ GeV $^2/c^2$, within the systematic errors of the data and models. This is somewhat

higher in Q^2 than for the unpolarized F_2 structure, supporting the conclusions of Ref. [8].

Turning to the examination of “local” duality for the proton, it can be seen in the upper left panel of Fig. 3 that in the “first” resonance region, dominated by the $\Delta(1232)$ resonance, the data have the opposite sign of the extrapolations of DIS models at low Q^2 . This is allowed by the spin-3/2 nature of the $\Delta(1232)$, and is expected due to the dominance of the M1 transition strength [25], as discussed above. What is interesting is that, while the data change sign at Q^2 near $1 \text{ GeV}^2/c^2$, the averaged values are significantly below the models even to the highest Q^2 of the present experiment, in spite of the fact that the $N \rightarrow \Delta(1232)$ transition form factor (FF) decreases more rapidly with Q^2 than, for example, the elastic FF or the $N \rightarrow S_{11}(1535)$ transition FF [25, 27] (a phenomena sometimes referred to as the “disappearing Δ ”). It is evident that the $\Delta(1232)$ has not yet completely disappeared at $Q^2 = 5 \text{ GeV}^2/c^2$.

In the second resonance region, two of the three known resonances [$P_{11}(1440)$ and $S_{11}(1535)$] contribute only to $\sigma_{1/2}$, while the third [$D_{13}(1520)$] contributes more to $\sigma_{1/2}$ than to $\sigma_{3/2}$ above $1 \text{ GeV}^2/c^2$ [26]. Therefore, it isn’t surprising that the proton data lie significantly above the DIS extrapolations in this narrow region of W .

In the “third” resonance region centered on 1.7 GeV , the $F_{15}(1680)$ is dominant at low Q^2 , but above about $1 \text{ GeV}^2/c^2$ other resonances are also important [26], such as the $S_{11}(1650)$, $S_{31}(1620)$, and $D_{33}(1700)$. The F_{15} contributes mainly to $\sigma_{3/2}$ at low Q^2 (i.e. negative g_1), but switches to $\sigma_{1/2}$ dominance at higher Q^2 [26]. The average over all of these resonances plus non-resonant background produces very good agreement between data and DIS models in this region, as might be expected from the parity-averaging arguments of Close and Isgur [7].

For completeness, we have also studied a fourth region centered on 1.9 GeV (for which there are a large number of poorly established resonances, difficult to distinguish from non-resonant contributions). In this case, the data lie slightly below the DIS models, although the significance is marginal when systematic errors are taken into account. It appears that much of the good agreement between data and models observed in the entire resonance region comes about from pairing the “first” and “second” resonance regions together, with further improvement from including the “fourth” region. This lends further support to the Close-Isgur model.

Again following Close and Isgur [7], one might expect DIS and resonance region data to

converge at lower values of Q^2 if the ground state elastic contribution is also included in the global duality averaging. The open circles in Fig. 2 include the elastic (quasi-elastic) contributions to the g_1 averages for the proton (deuteron), given by $G_E(Q^2)[G_E(Q^2) + \tau G_M(Q^2)]/2(1 + \tau)(x_h - x_l)$, where $\tau = Q^2/4M^2$. To evaluate the nucleon electric and magnetic form factors $G_E(Q^2)$ and $G_M(Q^2)$, we used a slightly modified version of the parameterization of Ref. [28]. For both the proton and the deuteron, the Q^2 -dependence with the elastic contribution more closely resembles the Q^2 -dependence of the models, down to values of Q^2 as low as $0.7 \text{ GeV}^2/c^2$, which is already pushing below the expected region of validity of $1 \text{ GeV}^2/c^2$ for the PDF fits. However, the magnitude of the data is of order 10% to 20% higher than the models. As mentioned above, high- x resummation corrections may well account for this difference. The result of pairing the $\Delta(1232)$ resonance (the lowest spin-3/2 ground state) with the elastic contribution (the lowest spin-1/2 ground state) is illustrated in the upper left panel of Fig. 3 for the proton. The elastic contribution, in the way we have treated it, over-compensates, resulting in power-law deviations at low Q^2 that lie well above the data, rather than well below. It appears that including the elastic contribution with the entire resonance region works much better than pairing it with the single $\Delta(1232)$ resonance.

In summary, we have used data for both the proton and deuteron to examine both “local” and “global” quark-hadron duality in g_1 . As was determined in previous studies [1, 8], g_1^p in the resonance region oscillates around extrapolations of NLO PDF fits to higher energy data, especially when target-mass corrections are taken into account. Averaged over the traditional resonance region ($W < 2 \text{ GeV}$), the data and fits agree within errors for $Q^2 > 1.7 \text{ GeV}^2/c^2$, a slightly higher value than observed for the spin-averaged structure function F_2 [8, 10]. Including the elastic contribution may extend the region of agreement to $Q^2 = 0.7 \text{ GeV}^2/c^2$, after consideration of the uncertainties due to high- x resummation. A similar effect was found in the unpolarized case [1, 10]. We find similar results for the previously unexamined g_1^d structure function as for g_1^p , indicating no large effects from different isospin projections. In terms of “local” duality, we find that in the $\Delta(1232)$ region, the proton data lie below the PDF fits, even for Q^2 values as large as $5 \text{ GeV}^2/c^2$, while the region centered on 1.5 GeV lies above the PDF fits for all Q^2 values studied. It appears that global duality is largely realized by summing over the four lowest-mass resonances. Since the Q^2 -dependence for the PDF fits and the data are remarkably similar above $Q^2 = 1.7 \text{ GeV}^2/c^2$, we conclude that

from the practical point of view, it is not unreasonable, with suitable averaging over W , to include data with $W > 1.58$ GeV and $Q^2 > 1.7$ GeV²/c² in future global NLO PDF fits, as long as the effects of TM and high- x resummation effects are taken into account. In the near future, high statistical accuracy data from the present experiment with 2.5 and 4.2 GeV electron energies, and additional data at 5.7 GeV, presently under analysis, will allow more precise studies, particularly for the deuteron.

We would like to acknowledge the outstanding efforts of the Accelerator, Target Group, and Physics Division staff that made this experiment possible. This work was supported by the U.S. Department of Energy, the Italian Istituto Nazionale di Fisica Nucleare, the U.S. National Science Foundation, the French Commissariat à l’Energie Atomique and the Korean Engineering and Science Foundation. The Southeastern Universities Research Association (SURA) operates the Thomas Jefferson National Accelerator Facility for the United States Department of Energy under contract DE-AC05-84ER40150.

* Electronic address: bosted@jlab.org; Corresponding author.

† Current address: Thomas Jefferson National Accelerator Facility, Newport News, Virginia 23606

‡ Current address: Massachusetts Institute of Technology, Cambridge, Massachusetts 02139-4307

§ Deceased

¶ Current address: University of New Hampshire, Durham, New Hampshire 03824-3568

** Current address: Moscow State University, General Nuclear Physics Institute, 119899 Moscow, Russia

†† Current address: Los Alamos National Laboratory, Los Alamos, New Mexico 87545

‡‡ Current address: Catholic University of America, Washington, D.C. 20064

§§ Current address: Physikalisches Institut der Universität Giessen, 35392 Giessen, Germany

¶¶ Current address: University of Massachusetts, Amherst, Massachusetts 01003

[1] W. Melnitchouk, R. Ent, C. Keppel, Phys. Rep. **406**, 127 (2005).

[2] E.D. Bloom and F.J. Gilman, Phys. Rev. Lett. **25**, 1140 (1970); Phys. Rev. D **4**, 2901 (1971).

[3] H. Georgi and H.D. Politzer, Phys. Rev. D **14**, 1829 (1976).

[4] O. Nachtmann, Nucl. Phys. **63**, 237 (1975).

- [5] J. Blümlein and A. Tkabladze, Nucl. Phys. **B553**, 427 (1999).
- [6] A. de Rújula, H. Georgi and H.D. Politzer, Ann. Phys. **103**, 315 (1975); Phys. Lett. B **64**, 428 (1976).
- [7] F.E. Close and N. Isgur, Phys. Lett. **B509**, 81 (2001); F.E. Close and W. Melnitchouk, Phys. Rev. C **68**, 035210 (2003).
- [8] N. Bianchi, A. Fantoni, and S. Liuti, Phys. Rev. D **69**, 014505 (2004).
- [9] S. Forte, G. Ridolfi, J. Rojo, M. Ubiali, Phys. Lett. B **635**, 313 (2006).
- [10] I. Niculescu, *et al.*, Phys. Rev. Lett. **85**, 1182 (2000); Phys. Rev. Lett. **85**, 1186 (2000).
- [11] C.E. Carlson and N.C. Mukhopadhyay, Phys. Rev. D **58**, 094029 (1998); Phys. Rev. D **41**, 2343 (1990).
- [12] G. Baum *et al.*, Phys. Rev. Lett. **43**, 2000 (1980).
- [13] K. Abe *et al.*, Phys. Rev. Lett. **78**, 815 (1997); Phys. Rev. D **58**, 112003 (1998).
- [14] A. Airapetian *et al.*, Phys. Rev. Lett. **90**, 092002 (2003).
- [15] R. Fatemi *et al.*, Phys. Rev. Lett, **91**, 222002 (2003).
- [16] J. Yun *et al.*, Phys. Rev. C **67**, 055204 (2003).
- [17] M. Hirai *et al.*, Phys. Rev. D **69**, 054021 (2004).
- [18] M. Gluck, E. Reya, M. Stratmann and W. Vogelsang, Phys. Rev. D **63**, 094005 (2001).
- [19] F. M. Steffens and W. Melnitchouk, Phys. Rev. C **73**, 055202 (2006).
- [20] K.V. Dharmawardane *et al.*, nucl-ex/0605028, submitted to Phys. Lett. 2006.
- [21] B.A. Mecking, *et al.*, Nucl. Instr. Meth., **503**, 513 (2003).
- [22] C.D. Keith *et al.*, Nucl. Instr. Meth. **501**, 327 (2003).
- [23] M.E. Christy, private communication for fit to data in: E94-110 Collaboration, Y. Liang *et al.*, nucl-ex/0410027, JLAB-PHY-04-45, submitted to Phys. Rev. Lett.
- [24] I. Niculescu, private communication for fit to data in Ref. [10].
- [25] K. Joo *et al.*, Phys. Rev. Lett. **88**, 122001 (2002); V.V. Frolov *et al.*, Phys. Rev. Lett. **82**, 45 (1999); M. Ungaro *et al.* hep-ex/0606042 (2006).
- [26] V. Burkert and T.S. Lee, Int. J. Mod. Phys. E13, 1035 (2004).
- [27] P. Stoler, Phys. Rep. 226, 103 (1993).
- [28] P. Bosted, Phys. Rev. C **51**, 409 (1995).

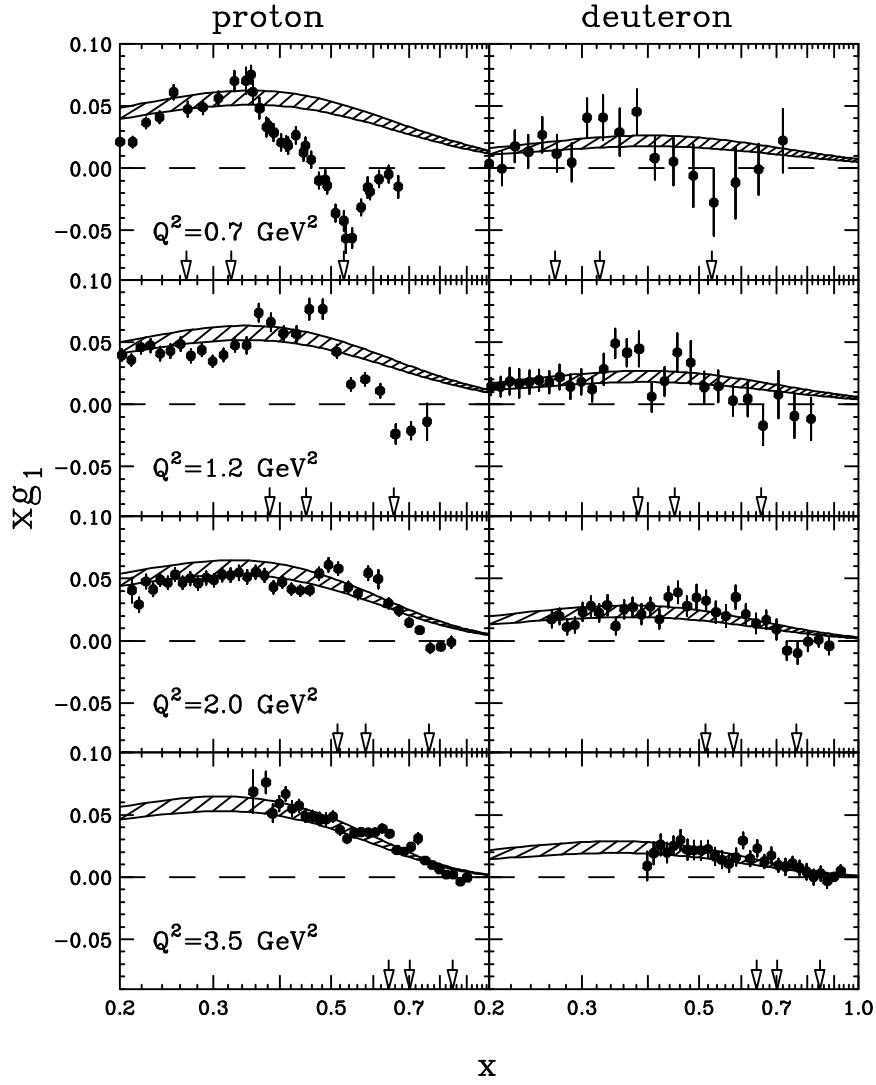


FIG. 1: Present data for proton $g_1^p(x, Q^2)$ (left panels) and deuteron $g_1^d(x, Q^2)$ (defined to be per nucleon, right panels) at four representative values of Q^2 . The errors include statistical and systematic contributions added in quadrature. The three arrows on each plot indicate the central kinematic position of the three prominent resonance regions at $W = 1.7, 1.5,$ and 1.23 GeV from left to right. The hatched band represents the range of g_1 predicted by modern NLO Parton Distribution Function (PDF) fits (GRSV [18] and AAC [17]) to high energy data, evolved to the Q^2 of our data and corrected for target-mass as described in the text.

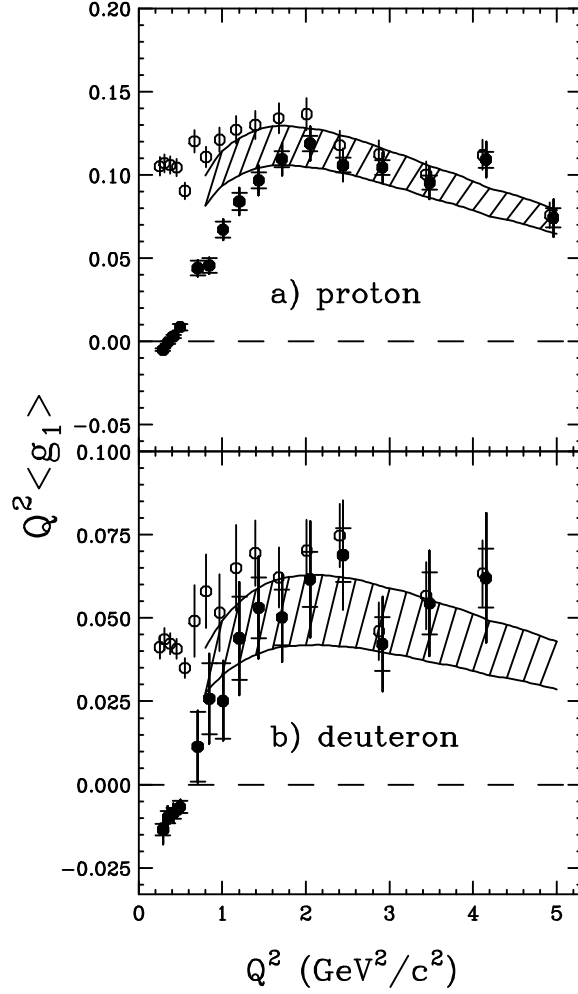


FIG. 2: The Q^2 -dependence of $Q^2 g_1(x, Q^2)$, averaged over a region in x corresponding to $1.08 < W < 2$ GeV (solid circles) for: a) proton; b) deuteron. The inner error bars reflect only statistical contributions, while the outer error bars include statistical and systematic components added in quadrature. The open circles represent our data after adding the contribution from ep elastic (ed quasielastic) scattering at $x = 1$ for the proton (deuteron). For clarity these results are slightly displaced in Q^2 , and the error bars include only statistical contributions. The hatched bands represent the range of the averages calculated from extrapolated NLO DIS fits, as in Fig. 1 (see text for details).

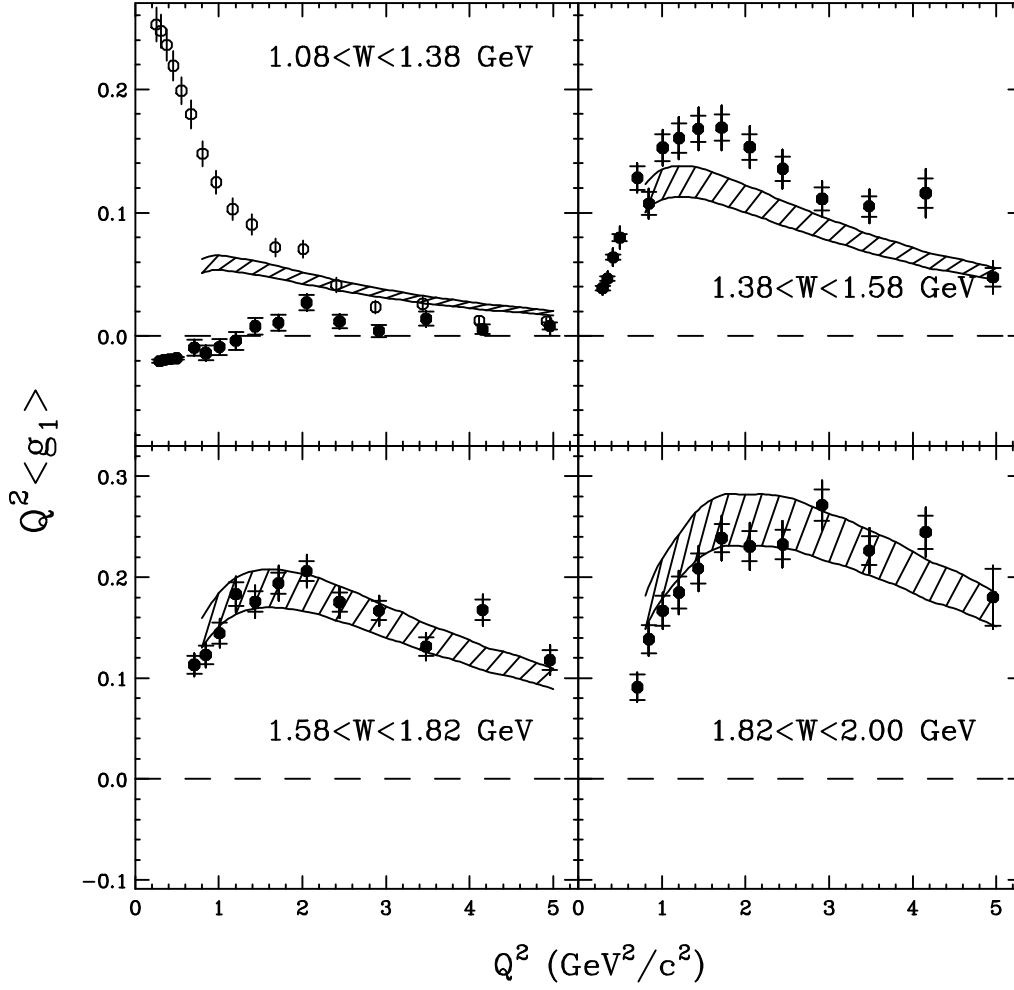


FIG. 3: The Q^2 -dependence of $Q^2 g_1(x, Q^2)$ for the proton, averaged over various regions of x . At each Q^2 , the x -range over which g_1 was averaged is determined by the corresponding range in W as indicated in each panel (see text). Symbols and curves as in Fig. 2.